Journal of NeuroVirology, 15: 300–311, 2009

ISSN 1355-0284 print / 1538-2443 online
DOI: 10.1080/13550280903030125

informa
healthcare

Cell-specific temporal infection of the brain in a simian immunodeficiency virus model of human immunodeficiency virus encephalitis

Katherine A Thompson,[1,2] John J Varrone,[3] Tanja Jankovic-Karasoulos,[1,2] Steven L Wesselingh,[2,4] and Catriona A McLean[1,2]

[1]Department of Anatomical Pathology, The Alfred Hospital, Melbourne, Victoria, Australia; [2]Department of Medicine, Monash University, Melbourne, Victoria, Australia; [3]Department of Molecular and Comparative Pathobiology, Johns Hopkins School of Medicine, Baltimore, Maryland, USA; and [4]Macfarlane Burnet Institute for Medical Research and Public Health, Melbourne, Victoria, Australia

Increasing evidence supports early brain infection by human immunodeficiency virus (HIV). Definitive temporal studies determining when and within which brain cells viral DNA is present are lacking. This study utilized simian immunodeficiency virus (SIV)-infected macaques sacrificed at days 10, 21, 56, and 84 post inoculation. Laser-microdissection isolated pure perivascular macrophage, parenchymal microglia, and astrocyte populations. Nested polymerase chain reaction (PCR) and sequencing determined the presence and characteristics of SIV V3 and V1 *env* DNA from each population. At day 10, SIV DNA was detected in perivascular macrophage and astrocytes but not parenchymal microglia. gp41 expression was restricted to perivascular macrophage. At day 21, SIV DNA was not detected in any cell type. At day 56, SIV DNA was detectable in perivascular macrophage from one of two macaques, with no gp41 expression detected. At day 84 (morphologic and clinical encephalitis), SIV DNA was detected in all cell types, gp41 was only detected in perivascular macrophage and parenchymal microglia. The neurovirulent molecular clone, SIV/17E-Fr, was the only genotype identified in the brain cell populations. Early, productive brain SIV infection was transient and restricted to trafficking perivascular macrophage. During the nonencephalitic stage, there was a period of time when no SIV DNA could be detected in the brain cell populations. SIV was then seen to reenter the brain via infected perivascular macrophage, leading to productive infection of brain parenchymal macrophage/microglia with a terminal phase of encephalitis. These data challenge current notions of a HIV reservoir within latently infected, semipermanent brain cells and has significant implications for the timing and design of therapies to prevent HIV encephalitis (HIVE). *Journal of NeuroVirology* (2009) **15,** 300–311.

Address correspondence to Dr. Katherine A. Thompson, Department of Anatomical Pathology, The Alfred Hospital, Commercial Road, Melbourne, Victoria, 3004, Australia. E-mail: Katherine.Thompson@med.monash.edu.au

The current address of Tanja Jankovic-Karasoulos is Institute of Medical and Veterinary Science, Hanson Institute, Adelaide, South Australia.

The current address of Steven L. Wesselingh is Faculty of Medicine, Nursing and Health Sciences, Monash University, Melbourne, Victoria, Australia.

This work was supported by an Australian National Health and Medical Research Council (NHMRC) grant (281215) to C.A.M. and S.L.W. K.A.T. was supported by a NHMRC Biomedical Postgraduate Scholarship (194342) and is currently a recipient of a NHMRC Peter Doherty Post-Doctoral Fellowship (415006).

The authors thank M. C. Zink, L. Gama, M. J. Churchill, and P. R. Gorry for helpful advice. Macaque brain tissues were kindly provided by M. C. Zink, with J. E. Anderson and A. Hasgrove providing assistance in tissue transportation and clinical data (Johns Hopkins School of Medicine, Baltimore, Mayland, USA). The authors also thank A. Gooey for assistance with processing tissue samples and C. Cherry for critical reading of the manuscript.

Received 18 December 2008; Revised 19 March 2009; accepted 10 April 2009.

Keywords: human immunodeficiency virus; simian immunodeficiency virus encephalitis; neuropathogenesis; laser microdissection

Introduction

The introduction of highly active antiretroviral therapy (HAART) has significantly decreased the incidence of acquired immunodeficiency syndrome (AIDS), human immunodeficiency virus encephalitis (HIVE), and of HIV-associated dementia (HAD) (Dore *et al*, 1999; Sacktor, 2002). HAART is frequently not initiated until well after acute infection when HIV is disseminated throughout the body, including the brain (Gray *et al*, 1996). Thus the virus may have already entered and established infection in the brain, resulting in a latent viral infection in long-lived cells, sequestered from immune surveillance. The brain may then act as a reservoir of latent virus that current therapeutics are unable to eliminate, and that could reactivate later in disease. Additionally, ongoing persistent infection of brain cells may result in the inability of the infected cells to perform normal functions critical for brain functioning (Overholser *et al*, 2003).

Limited studies of acute HIV infection suggest that virus enters the brain during acute infection (Bell, 2004; Bell *et al*, 2006; Gonzalez-Scarano and Martin-Garcia, 2005), but it is not clear whether virus that enters the brain during acute infection persists there for life or whether this is cleared by the host and HIVE develops as a result of later introduction of new virus into the brain. It is crucial to understand the events that lead to establishment of virus in the brain and the eventual development of HIVE. Studies of HIV infection of the human brain are necessarily limited by difficulty in accessing acutely infected individuals and the inaccessibility of the human brain for sampling during early infection in life. SIV-infected macaques may provide a useful model to study when and in which brain cells retroviral infection occurs. Macaques can be inoculated with well-characterized virus strains to identify specific viral genes that are important in the development of organ-specific disease, such as the demonstration that *env* and *nef* genes contain molecular determinants of neurovirulence (Mankowski *et al*, 1997). Body fluid and tissues can be repeatedly sampled at different times during the course of infection to measure virus replication and evaluate the hosts' immune responses. Finally, infected animals can be euthanized at different stages of infection to reconstruct the complete kinetic picture of infection. Previous work utilizing a SIV model combined immunohistochemistry (IHC) and *in situ* hybridisation to show that SIV infection was localized to perivascular macrophage at the earliest stage and was found in perivascular macrophage and microglial cells scattered through the brain parenchyma at later stages (Chakrabarti *et al*, 1991). Another study analyzed envelope sequences from individual brain multinucleated giant cells of simian immunodeficiency virus (SIV) encephalitic macaques; however, interpretation of temporal pathogenesis is limited in that the study analyzed only six multinucleated giant cells (MNGCs) from one macaque with end-stage disease (Ryzhova *et al*, 2002).

Clements *et al* (1994) previously developed a SIV/macaque model that causes consistent, accelerated HIVE in $>90\%$ of infected animals by 84 days post inoculation (Clements *et al*, 1994; Zink *et al*, 1997, 1998). Pigtailed macaques (*Macaca nemestrina*) are inoculated with a neurovirulent molecular clone, SIV/17E-Fr (Flaherty *et al*, 1997) and an immunosuppressive biological isolate, SIV/DeltaB670, that consists of at least 20 different genotypes (as determined by sequencing of the V1 region of *env*) (Babas *et al*, 2003). The high incidence of HIVE in this model provides an opportunity to correlate host and viral events in the brain during the acute infection with the later development of HIVE (Zink *et al*, 1997, 1998, 1999).

In this study, laser microdissection (LM) was utilized to isolate specific brain cell populations from macaques infected with SIV and sacrificed at different time points following infection. Morphologic analysis of the tissue sections at each time point was performed to assess for evidence of encephalitis. Triple-nested polymerase chain reaction (PCR) was utilized to determine the presence and genetic characterisation of SIV V3 *env* DNA sequences from the cell populations. This enabled examination of which cells were infected as early as 10 days post SIV infection, and how the infection in cells proceeds over the 3-month time span. Additionally, by cloning and sequencing the V1 envelope region of SIV DNA, it could be determined which of the inoculated SIV genotypes were present in the brain cells and whether they differed between cell populations.

Results

Brain histopathology

IHC and hematoxylin and eosin (H&E) stains performed on the brain sections were microscopically examined by a neuropathologist (C.A.M.) (Table 1). At day 10 post SIV inoculation, SIV gp41 positivity (indicative of productive infection by SIV) was only detected in perivascular macrophage. A moderate inflammatory response was noted (Figure 1A and B). At day 21, SIV gp41 IHC was not detected in

Table 1 Viral loads, immunohistochemical detection, and PCR detection of SIV DNA

Macaque	Day of infection	Plasma viral load (SIV copy Eq/ml)	CSF viral load	Macrophage (CD68 IHC)	Microglia (CD68 IHC)	Astrocytes (GFAP IHC)	SIV (gp41 IHC)	SIV gp41+ve cells	SIV V3 *env* DNA[b]		
				(−, +, ++, +++, +++)[a]					A	PVM	Mi
									(✓ or ×)		
MV672	10	27,000,000	43,000	+++	++	+	++	PVM	✓	✓	×
MF4C	10	<300	<300	+++	++	+	++	PVM	✓	✓	×
MV698	21	11,000,000	5200	++	++	+	−		×	×	×
MV390	21	3,600,000	1800	++	++	+	−		×	×	×
M879	56	6,100,000	2500	+	+	+	−		×	×	×
M369	56	6,000,000	17,000	+	+	+	−		×	✓	×
BM03	84	42,121,833	813,900	+++	+++	++	+++	PVM, Mi	✓	✓	✓
BI55	84	1,895,420	581,510	+++	+++	++	+++	PVM, Mi	✓	✓	✓
98P005	SIV-ve	0	0	+	−	+	−		×	×	×
98P006	SIV-ve	0	0	+	−	+	−		×	×	×

[a]Qualitation of immunohistochemical detection of brain cells; macrophage, microglia, and astrocytes and SIV productively infected brain cells. - = no positive cells; + = scant; ++ for between + and +++; +++ = many; and ++++ = numerous positive cells. A = astrocytes; PVM = perivascular macrophage; Mi = microglia; SIV-ve = SIV negative macaque.
[b]Detection of SIV-1 V3 *env* DNA from microdissected cell populations; astrocytes, macrophage, and microglia by highly sensitive triple-nested PCR. ✓ = presence or × = absence of SIV DNA.

perivascular macrophage, parenchymal microglia, or astrocytes (Figure 1D). Minimal inflammatory response was seen (Figure 1C). A minimal inflammatory response was also seen at day 56 (Figure 1E). SIV gp41 IHC was not detected in perivascular macrophage, parenchymal microglia, or astrocytes (Figure 1F). At day 84, a marked inflammatory response seen (Figure 1G) with a secondary astrocytic reaction (Table 1). SIV gp41 positivity was detected in numerous perivascular macrophage and parenchymal microglia (Figure 1H). The findings at day 84 were those of SIVE.

Presence and genetic characterisation of SIV V3 and V1 env DNA sequences from brain cell populations of SIV-infected macaques

Triple-nested PCR was utilized to determine the presence of SIV V3 *env* DNA within genomic DNA extracted from the cell populations—perivascular macrophage, parenchymal microglia, and astrocytes—from SIV-infected macaques at days 10, 21, 56, and 84. The sensitivity of the triple-nested PCR was determined to be one or more copies of SIV V3 *env* DNA per reaction. Integrity of DNA samples was established by performing a similar highly sensitive PCR analysis of cellular GAPDH levels; we were able to amplify GAPDH in all samples. Neurons were microdissected from cortical regions adjacent to white matter where perivascular macrophage, parenchymal microglia, and astrocytes were isolated. SIV DNA could not be detected in the neurons of the infected macaques examined (data not shown), as previously described (Thompson *et al*, 2004). Figure 2 shows PCR amplification of SIV V3 *env* DNA from LM cell populations from macaques at the four time points post inoculation with SIV. Table 1 summarises the PCR results and includes previously quantified plasma and cerebrospinal fluid (CSF) viral loads of the macaques (Babas *et al*, 2006). The SIV V3 *env* region was successfully amplified from astrocyte and perivascular macrophage populations from both macaques at day 10. At day 21, there was no detection of SIV V3 *env* DNA in any of the cell populations from either macaque. At day 56, SIV V3 *env* DNA was only detected in the perivascular macrophage of macaque M369. At day 84, SIV V3 *env* DNA was detected in perivascular macrophage, astrocytes and parenchymal microglia from both macaques. SIV V3 *env* DNA could not be detected in perivascular macrophage, astrocytes, and parenchymal microglia from either of the SIV negative macaques. The results demonstrate that SIV V3 *env* DNA was present *in vivo* in astrocytes and perivascular macrophage during acute SIV infection at day 10; however, by day 21, SIV V3 *env* DNA was absent or below the level of detection in these cell populations. At day 56, as the macaques progress towards terminal encephalitis, SIV V3 *env* DNA was detected only in perivascular macrophage. At day 84, both macaques had SIVE and SIV V3 *env* DNA was detected in all three cell populations, perivascular

macrophage, astrocytes, and parenchymal microglia. The detection of SIV V3 *env* DNA from genomic DNA extracted from nondissected tissue section homogenates of the SIV-infected macaques were also analyzed. Viral DNA was detected at days 10 and 84 in both macaques, in one of the two macaques at day 56, and no viral DNA was detected at day 21. These results mirrored those of the laser-dissected brain cell populations (data not shown).

The PCR products of at least three independent PCR reactions were pooled and cloned. Multiple SIV V3 and V1 *env* clones were obtained from the brain cell populations from each macaque and sequenced. Sequences were aligned against the SIV viruses initially inoculated into the macaques, SIV/DeltaB670 and SIV/17E-Fr (Figure 3A). Sequencing confirmed the PCR results of SIV V3 *env* DNA detection. Sequencing of the V1 region of *env* was performed to distinguish between SIV/17E-Fr and the 20 different genotypes of SIV/DeltaB670 (Babas *et al*, 2003). The neurovirulent inoculating SIV molecular clone, 17E-Fr, was the only genotype identified in all three-cell populations (Figure 3B).

Discussion

This study utilized a SIV model with highly sensitive PCR to detect SIV V3 and V1 *env* DNA from laser-microdissected brain cell populations at specific time points of sacrifice to determine the temporal relation of SIV infectivity. The results show that the virus enters early into the brain with productive infection of perivascular macrophage and nonproductive infection of astrocytes and that this occurs at a time of encephalitic changes and detectable high plasma and CSF viral loads. Following the acute infection, virus becomes undetectable in perivascular macrophage, parenchymal microglia, and astrocytes but is detected again at later time points.

Perivascular macrophage traffic through the perivascular space of the brain via the systemic circulation and are in a state of constant turnover. Turnover of perivascular macrophage can be detected in noninflammatory conditions within as little as 24 h and is accelerated in inflammatory conditions such as viral infections (Bechmann *et al*, 2001; Kim *et al*, 2006; Williams *et al*, 2001). The perivascular space represents the central nervous system (CNS) equivalent of the lymphatic space. Within this space, the perivascular macrophage are equipped to recognise antigen and present it to T cells (Galea *et al*, 2005; Subramanian *et al*, 2001). The inability to detect SIV DNA within the brain cell populations parallels both the relatively decreased plasma and CSF viral load and undetectable viral RNA in brains of macaques at days 21 and 56 after inoculation, as previously described (Clements *et al*, 2002). With lower levels of viremia, it is possible that fewer infected perivascular macrophage traffic to the brain; however, within the sensitivity of our work, no SIV DNA could be detected within these macrophage (Williams *et al*, 2001). A lack of viral DNA in perivascular macrophage suggests that at this time point, these circulating macrophage cannot act in a 'Trojan horse' capacity (Clay *et al*, 2007).

How HIV infects astrocytes *in vivo* has not been clearly defined, although a recent study implicates the human mannose receptor in astrocyte entry of HIV (Liu *et al*, 2004). Overholser *et al*, 2003, using SIV Nef immunohistochemistry and the SIV model, established that astrocytes were productively infected in macaques during acute SIV infection (10 days post inoculation) and during terminal infection (84 days post inoculation) but were negative for SIV Nef protein at days 21 and 56.

Inability to detect SIV DNA in astrocytes during stages of nonencephalitic pathology (days 21 and 56) suggests that nonproductively infected cells may be eliminated. The mechanism for this is unclear but it may relate to apoptosis of the nonproductively infected astrocyte or it may involve a CD8 lymphocyte–directed immune response, recognizing and lysing astrocytes expressing viral protein (Clements *et al*, 2002; Thompson *et al*, 2001). Another proposed mechanism is that virus is being destroyed through phagocytic activity of the astrocyte. Phagocytic activity is one of the physiological functions of astroglial cells, particularly in response to inflammation (Iacono and Berria, 1999; Kalmar *et al* 2001; Speth *et al*, 2005). Clarke *et al* (2006) infected multiple astrocytoma cell lines with cell-free HIV. Consistent with the results of recent studies, they observed uptake of HIV into vesicle-like compartments with limited reverse transcription (Clarke *et al*, 2006). The size of these vesicles suggests that the virus may be internalized by macropinocytosis or phagocytosis (Sieczkarski and Whittaker, 2002). These results are consistent with the involvement of the mannose receptor on astrocytes for virus entry. Few, if any, of the HIV virions taken up by the mannose receptor pathway are able to escape from degradation within the endosome/lysosomes and proceed to the typical postentry pathway of HIV infection (Liu *et al*, 2004). Phagocytosis of HIV by astrocytes may occur during acute infection, whereas the widely accepted pathway involving restricted virus replication in astrocytes may predominately occur at terminal infection (Churchill *et al*, 2006).

The microglia or resident brain macrophage have an extended half-life and exist within the brain neuropil. These cells are a stable population and are resident in the brain from birth, forming a dense reticular network with an anatomic location and morphologic appearance distinct from perivascular macrophage (Kreutzberg *et al*, 1997). No detectable

SIV DNA was found in the microglial population until day 84 and there was no evidence of active production of virus until the same time point. The infection of perivascular macrophage and not parenchymal microglia at the early time point of infection may account for the early productive viral infection, disappearance, and reappearance of SIV in the brain.

At day 56, when the plasma viral load rises and the peripheral CD4 count decreases (Chris Zink, personal communication), SIV DNA is again detectable in the perivascular macrophage. This suggests that reentry of virus into the brain is via perivascular macrophage. Thus the perivascular macrophage can then be seen to be the 'Trojan horse' (Clay *et al*, 2007). By day 84, there is extensive spread of infection, not only to the perivascular macrophage but also to parenchymal microglia and astrocytes, and an inflammatory response is seen within the brain parenchyma. These changes occur in parallel with a marked rise in the plasma and CSF viral load.

Our results suggest that viral strains are transmitted from trafficking cells to susceptible cells within the brain parenchyma. For example, astrocytes are infected in the initial infection but this is a nonproductive and nonsustainable infection. During the early stages of infection, viral replication in the brain is limited to the perivascular macrophage and modified by an intact host immune response. Once the host's immune system deteriorates and uncontrolled systemic viral replication occurs, viral replication in the brain again ensues. This is initially reflected by reentry of replicating virus within the perivascular macrophage and followed by spread of infectivity and neurotropism to astrocytes and microglia at a time of activation of an inflammatory response with production of cytokines, influx of inflammatory cells, and alteration of the parenchymal microenvironment.

If the SIV model parallels HIV infection of the brain, prevention of reinfection by suppression of a plasma viral load would be essential in preventing subsequent intraparenchymal brain pathology. Specific targeting of systemically infected macrophage may prevent those that circulate into the CNS perivascular space from allowing brain infection.

A previous study utilizing the same macaque model, in contrast with the current study, demonstrated that SIV DNA persisted in the brain at steady-state levels throughout infection (Clements *et al*, 2002). In our study, genomic DNA extracted from nondissected tissue section homogenates at each time point were also analyzed for SIV DNA and its presence or absence paralleled our findings of dissected brain cell populations at each time point. Our work utilized the approach of studying small numbers of animals (two per time point) and specifically studied 800 cells of each population per time point. Previous work detecting SIV DNA used larger numbers of homogenized brain samples (including basal ganglia, cortex, and cerebellum), but this work did not discriminate cell-specific SIV infection versus total brain infection (Babas *et al*, 2003, 2006; Clements *et al*, 2002). Without cell specificity of infection, it is not possible to determine whether any positive finding in a tissue homogenate represents a circulating infected cell or an infected brain cell. Hence the absence of SIV DNA in brain cell populations at certain time points in our study may either reflect a lack of sensitivity (the sensitivity of our PCR was determined to be one or more copies of SIV V3 *env* DNA per reaction, as discussed above) or represent an alternate viral DNA cellular source; e.g., from infiltrating lymphocytes within the perivascular space in white matter homogenates (Clements *et al*, 2002), endothelial cells (Mankowski *et al*, 1994), fragments of choroid plexus (Petito *et al*, 1999), or neural progenitor cells (Rothenaigner *et al*, 2007; Schwartz *et al*, 2007).

SIV/17E-Fr was the only genotype identified in the three brain cell populations in each of the macaques. Previous work utilizing the same macaque model identified the neurovirulent molecular clone SIV/17E-Fr as the predominant genotype detected in brain DNA, with an over 95% frequency of detection in the basal ganglia (Clements *et al*, 2002). SIV/17E-Fr is a dual-tropic molecular clone that preferentially infects macrophages and causes encephalitis. It contains genetic determinants for neuroinvasion, neurotropism, and neurovirulence and as such may already be highly efficient at infecting the studied cell populations without the requirement for recombination. Another study suggests that the envelope from SIV/17E-Fr interacts with CCR5 in a CD4-independent manner, and changes in the transmembrane protein of this virus are important components that contribute to neurovirulence in SIV (Bonavia *et al*, 2005).

Figure 1 Photomicrographs of immunohistochemically stained sections from the subcortical white matter of macaques. (**A**) 10 days post inoculation with SIV, showing moderate macrophage/microglial response; immunoreaction CD68 × 200 (arrowhead points to ramified parenchymal microglial cells). (**B**) 10 days post inoculation with SIV, showing visible SIV gp41 positivity within macrophage in the perivascular space; immunoreaction SIV gp41 × 200. (**C**) 21 days post inoculation with SIV, showing minimal macrophage/microglial response; immunoreaction CD68 × 200 (arrowhead points to scant ramified parenchymal microglial cells). (**D**) 21 days post inoculation with SIV, showing no evidence of SIV gp41 positivity; immunoreaction SIV gp41 × 200. (**E**) 56 days post inoculation with SIV, showing negligible macrophage/microglial response; immunoreaction CD68 × 200 (arrowhead points to scant perivascular macrophage). (**F**) 56 days post inoculation with SIV, showing no evidence of SIV gp41 positivity, immunoreaction SIV gp41 × 200. (**G**) 84 days post inoculation with SIV, showing a marked macrophage/microglial response; immunoreaction CD68 × 200 (arrowhead points to activated ramified parenchymal microglial cells). (**H**) 84 days post inoculation with SIV, showing marked SIV gp41 positivity within macrophage both in the perivascular space and within the parenchyma; immunoreaction SIV gp41 × 200.

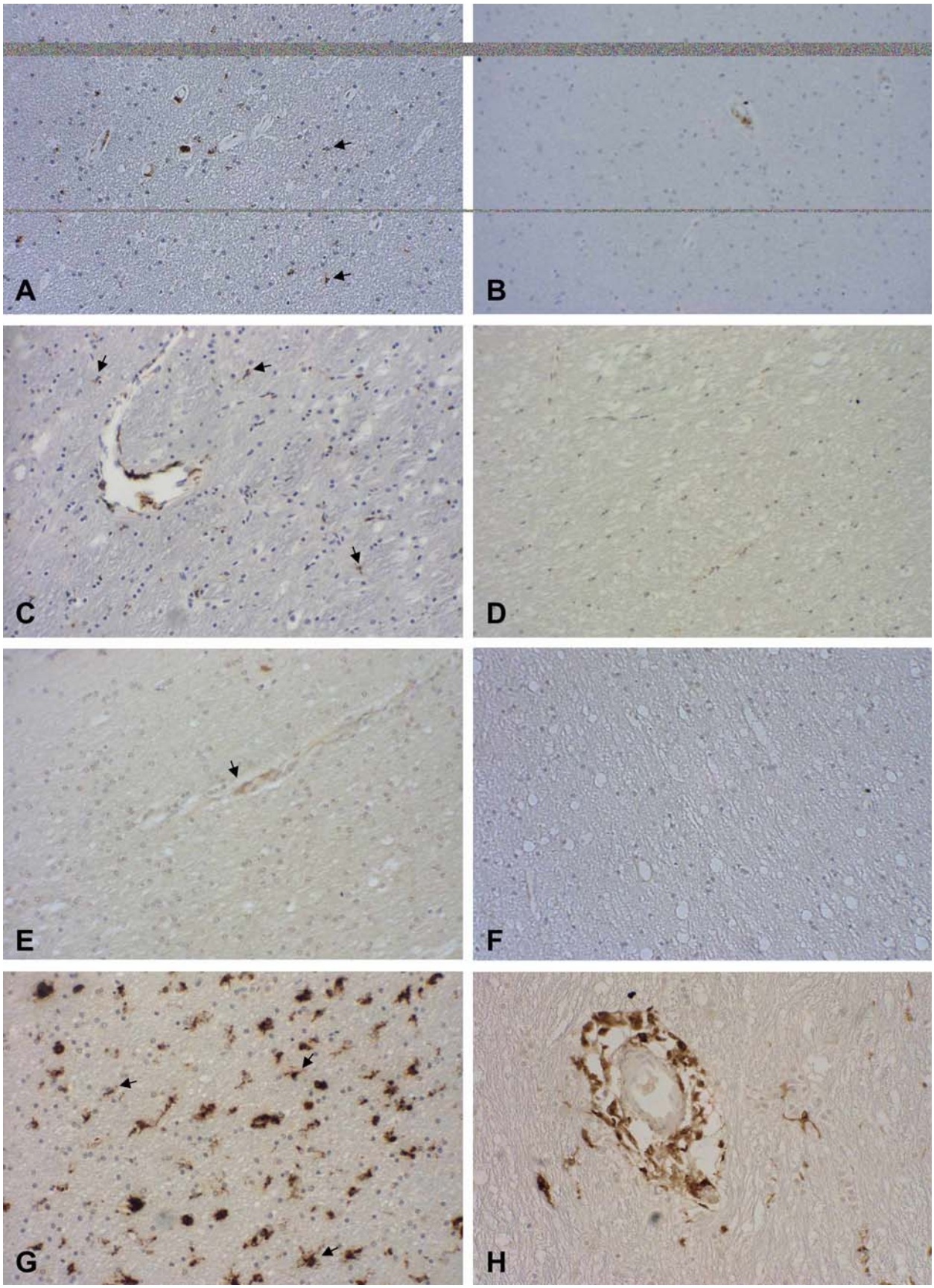

Figure 1 (*Continued*)

This SIV macaque model is unique because in 3 months it delineates the kinetics of SIV from acute infection to terminal disease. In combination with the ability to microdissect pure cell populations from specific regions of the brain and a triple-nested

Figure 2 Representative images of PCR amplifications of SIV V3 *env* DNA from cell populations microdissected from macaque brain tissue at the four time points post inoculation with SIV. SIV V3 *env* DNA PCR resulting in three rounds of PCR products (262, 215, and 169 bp). SIV V3 *env* DNA was not consistently detected in PCR amplification from samples in which there was low levels of virus. For this reason, cell populations were collected in duplicate (e.g., two collections of astrocytes per macaque) and the triple-nested PCR was performed on each duplicate cell population at least three times to increase the frequency of detection. Not every PCR amplification from DNA of cell populations is illustrated in the figure. Results of PCR amplifications of SIV V3 *env* DNA from all cell populations is in Table 1 and sequencing results in Figure 3A. (**A**) 10 days post inoculation with SIV. Lane 1, Negative PCR control (water as DNA template). Lane 2, Negative PCR control (water as DNA template) carried through three rounds of PCR. Lane 3, MV672 astrocytes. Lane 4, MV672 astrocytes (duplicate). Lane 5, MV672 macrophage. Lane 6, MV672 macrophage (duplicate). Lane 7, MV672 microglia. Lane 8, MF4C astrocytes. Lane 9, MF4C astrocytes (duplicate). Lane 10, MF4C macrophage. Lane 11, MF4C macrophage (duplicate). Lane 12, MF4C microglia. Lane 13, BI55 macrophage (day 84). Lane 14, BI55 DNA extracted from homogenized sample (positive control) (day 84) (over amplification results in PCR product not running through gel). (**B**) 21 days post inoculation with SIV. Lane 1, Negative PCR control (water as DNA template). Lane 2, 98P006 (SIV negative macaque) astrocytes. Lane 3, 98P006 (SIV negative macaque) macrophage. Lane 4, MV390 astrocytes. Lane 5, MV390 macrophage. Lane 6, MV390 macrophage (duplicate). Lane 7, MV390 microglia. Lane 8, MV698 astrocytes. Lane 9, MV698 astrocytes (duplicate). Lane 10, MV698 macrophage. Lane 11, MV698 macrophage (duplicate). Lane 12, MV698 microglia. Lane 13, BM03 astrocytes (day 84). Lane 14, BI55 macrophage (day 84). Lane 15, MV390 DNA extracted from homogenized sample. Lane 16, MV698 DNA extracted from homogenized sample. Lane 17, BM03 DNA extracted from homogenized sample (positive control) (day 84) (over amplification results in PCR product not running through gel). Lane 18, SIV plasmid p239 SpE3' (positive control). Lane 19, Negative PCR control (water as DNA template) carried through three rounds of PCR. (**C**) 56 days post inoculation with SIV. Lane 1, Negative PCR control (water as DNA template). Lane 2, Negative PCR control (water as DNA template) carried through three rounds of PCR. Lane 3, 98P005 (SIV negative macaque) astrocytes. Lane 4, 98P005 astrocytes (duplicate). Lane 5, 98P005 macrophage. Lane 6, 98P005 macrophage (duplicate). Lane 7, M369 astrocytes. Lane 8, M369 astrocytes (duplicate). Lane 9, M369 macrophage. Lane 10, M369 macrophage (duplicate). Lane 11, M879 astrocytes. Lane 12, M879 astrocytes (duplicate). Lane 13, M879 macrophage Lane 14, M879 macrophage (duplicate). Lane 15, BM03 macrophage (day 84). Lane 16, BM03 DNA extracted from homogenized sample (positive control) (day 84) (over amplification results in PCR product not running through gel). Lane 17, SIV plasmid p239 SpE3' included in third round as MW (band size) indicator. (**D**) 84 days post inoculation with SIV. Lane 1, Negative PCR control (water as DNA template). Lane 2, BI55 macrophage. Lane 3, BI55 macrophage (duplicate). Lane 4, BI55 astrocytes. Lane 5, BI55 astrocytes (duplicate). Lane 6, BM03 macrophage. Lane 7, BM03 macrophage (duplicate). Lane 8, BM03 astrocytes. Lane 9, BM03 astrocytes (duplicate). Lane 10, BM03 DNA extracted from homogenized sample (positive control). Lane 11, BI55 DNA extracted from homogenized sample (positive control) (over amplification results in PCR product not running through gel). Lane 12, BM03 microglia. Lane 13, SIV plasmid p239 SpE3' (positive control). Lane 14, Negative PCR control (water as DNA template).

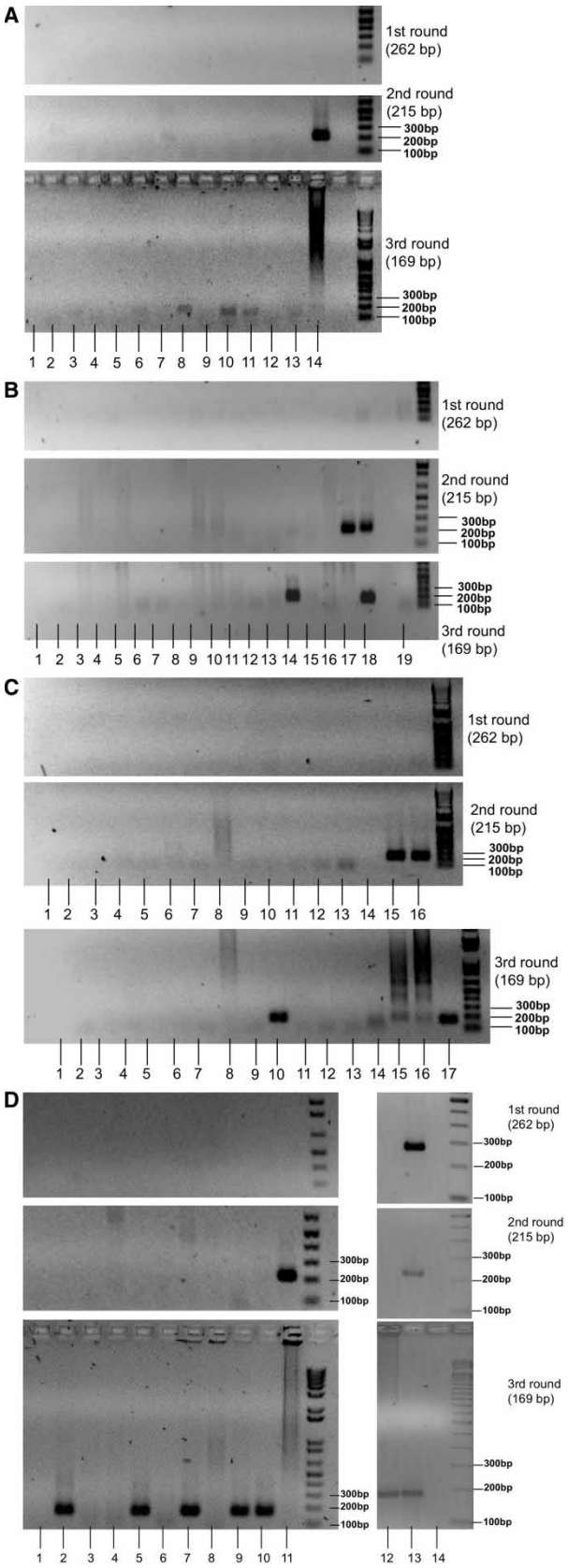

Figure 2 (*Continued*)

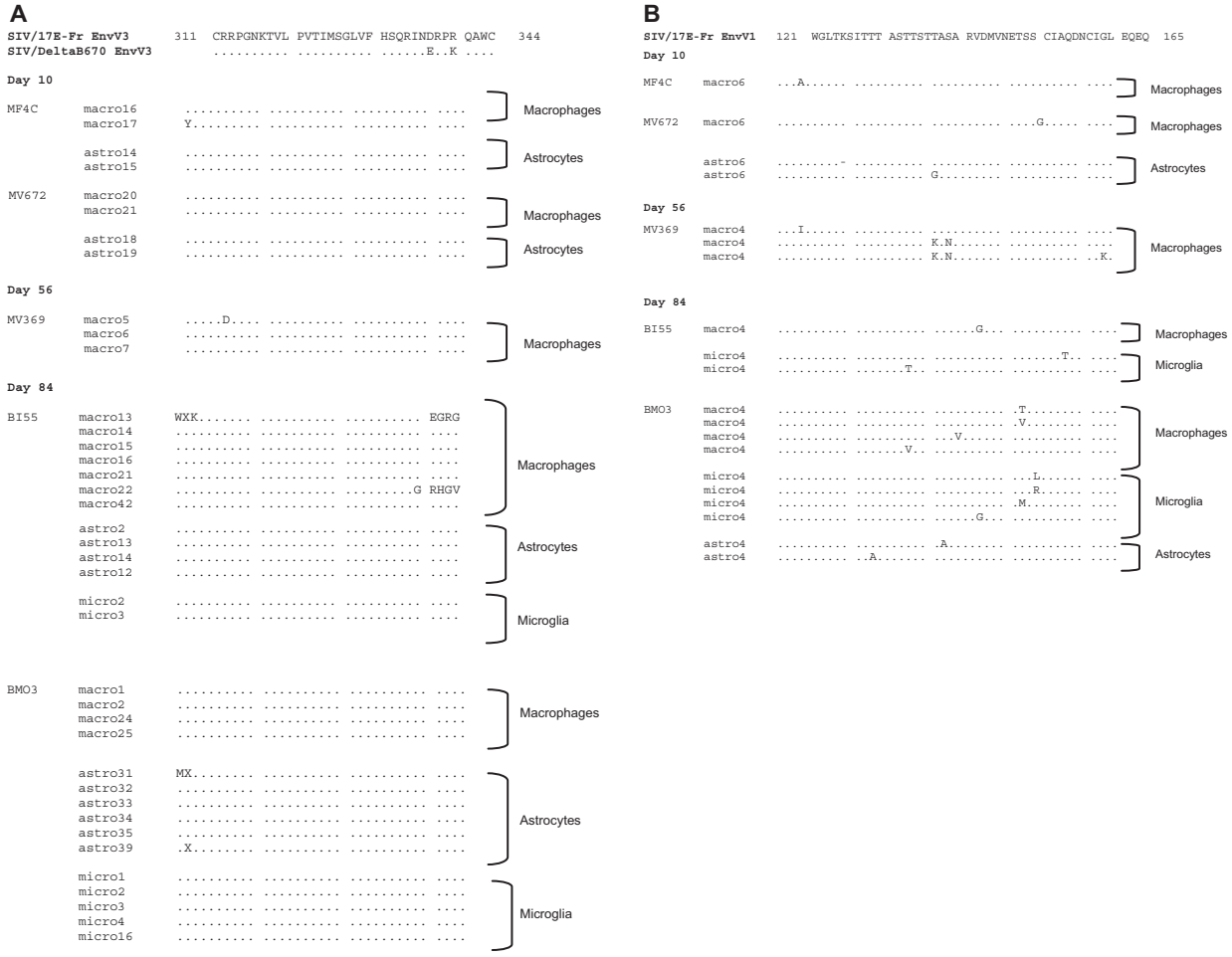

Figure 3 (**A**) Amino acid sequence alignment of SIV V3 *env* DNA cloned from the PCR products of LM isolated brain cell populations from macaques, 10 to 84 days post inoculation with SIV. (**B**) Corresponding amino acid sequence alignment of SIV V1 *env* DNA identifying the variations of SIV/17E-Fr. DNA sequences for V1 regions of clones isolated from astrocytes at day 10 for macaque MF4C and at day 84 for macaque BI55 were not detected and are therefore not in the sequence alignment of SIV V1 *env* DNA.

PCR strategy, this study has achieved a specificity and sensitivity not previously possible. The added advantage of isolation of DNA by laser microdissection is that the viral DNA can be sequenced to determine differences in viral DNA in different cell types, with potential to enhance an understanding of intracellular HIV access.

This temporal study examined the detection of SIV DNA in specific brain cell populations in combination with a morphologic analysis for encephalitis. After the acute infection, during the nonencephalitic stage, there was no SIV reservoir detectable in perivascular macrophage, parenchymal microglia, and astrocytes until progressive immunocompromise resulted in extensive SIV infection of perivascular macrophage, parenchymal microglia, and astrocytes in parallel with increased peripheral viral replication. These findings may contribute to improvements in the design and timing of preventative therapeutic measures aimed against the development of HIVE.

Materials and methods

Infection of macaques with SIV

The model consists of pigtailed macaques coinoculated with a neurovirulent molecular clone SIV/17E-Fr and virus strain, SIV/DeltaB670, which consistently and rapidly results in SIVE (Clements and Zink, 1996; Zink *et al*, 1998). Production of these viral stocks is detailed in Clements *et al* (1994). Three- to 5-year-old pigtailed macaques were intravenously inoculated with a mix of the two virus stocks. We utilized fixed brain tissue blocks of two macaques euthanased at each of four time points, 10, 21, 56, and 84 days post inoculation, in accordance with federal guidelines and institutional policies. At euthanasia, macaques were perfused with sterile saline to remove blood from the vasculature, thus allowing the accurate determination of viral genotypes in the brain parenchyma. Two SIV-uninfected macaques were used as controls.

Cell identification

Five-micron sections from STF-fixed (Streck Laboratories, Omaha, Nebraska), paraffin-embedded tissue blocks from the frontal cortex incorporating subcortical white matter, and basal ganglia, at the level of the anterior putamen were mounted on ''Superfrost plus'' charged glass slides (Fisher Scientific, Ontario, Canada). Sections were deparaffinized and morphologic examination in conjunction with IHC was performed on the brain tissue sections for the detection of astrocytes, macrophages, microglia, and SIV gp41 protein. A rabbit anti-human glial fibrillary acidic protein (GFAP) polyclonal antibody was used at a dilution of 1/50 for the detection of astrocytes (Zymed, San Francisco, CA). A mouse anti-human CD68 monoclonal antibody was used at a dilution of 1/200 for the detection of both perivascular macrophage and parenchymal ramified microglial cells (Clone KP1, Dako, Glostrup, Denmark). Perivascular macrophages were distinguishable by their round shape, with abundant cytoplasm and round nuclei with generally discrete cell borders that were seen outside the vessel walls, within Virchow-Robin spaces. Ramified parenchymal microglia were distinguished as cells with slender, elongated nuclei, ramified cytoplasmic processes, and a rod-shaped nucleus within the neuropil. Activated parenchymal microglial cells displayed up-regulated expression of the CD68 antigen, with more prominent ramification of processes and a more oval nucleus (Anthony *et al*, 2005; Hulette *et al*, 1992; Williams *et al*, 2001). A $SIV_{mac}251$ gp41 monoclonal antibody was used at a dilution of 1/400 for the detection of SIV protein (clone KK41; obtained from Karen Kent and Caroline Powell though the AIDS Research and Reference Reagent Program). Antibodies were used with the avidin-biotin complex method and a diaminobenzidine (DAB) hydrogen peroxide product as the colorimetric substrate. The gp41 antibody IHC required an antigen retrieval pretreatment of microwaving in sodium citrate buffer, 0.1 M (pH 6.0) (Laast *et al*, 2007). The CD68 antibody IHC required an antigen retrieval pretreatment of proteinase K (Dako). Routine H&E counterstains were performed on the sections to provide morphologic detail. The IHC-stained sections on slides, lacking coverslips, were dried in a fume hood for 20 to 30 min. These were stored in a desiccator overnight and laser dissection was performed the following day.

Laser microdissection

Perivascular macrophage, parenchymal microglia, and astrocytes within frontal subcortical white matter were laser dissected from the uncovered IHC-stained sections on slides and collected as pure cell populations for subsequent analysis. The PALM Microlaser system (P.A.L.M Mikrolaser Technologie) was utilized for the laser dissection. By combining the intense focal cutting tool with substage robotics, the laser beam was positioned to cut around the selected area on the tissue section and microdissect single cells, creating a clear-cut gap between the selected and nonselected areas. Once the cells of interest were isolated, the high energy generated by the focused laser light was used to catapult the dissected cells into a cap of a regular Eppendorf-type tube. Using this technology, the PALM was able to microdissect and capture cells without the use of manual manipulation, preventing contamination (Schuetze *et al*, 1997).

At least 200 cells, spanning the entire tissue section (or serial sections if required), were collected from each of the three cell populations in duplicate from each macaque (Thompson *et al*, 2004; Trillo-Pazos *et al*, 2003). Neurons dissected from overlying cortical regions served as negative internal controls, as previously described (Thompson *et al*, 2004). Genomic DNA was extracted from the cells using a PicoPure DNA extraction kit (Arcturus, Mountain View, CA). Genomic DNA from a 6-micron section of frontal cortex, including subcortical white matter and incorporating anterior putamen, per macaque, was also extracted using a MagneSil genomic, fixed-tissue DNA purification kit (Promega, Madison, WI). Both extractions were performed according to the manufacturer's protocol.

PCR amplification of SIV V3 env *DNA*

A triple-nested PCR was performed on DNA extracted from the cell populations to amplify SIV V3 *env* DNA sequences. V3 *env* sequences were amplified from genomic DNA prepared from LM-captured cell populations. Expand high-fidelity DNA polymerase (Roche Diagnostics, Basel, Switzerland) was used to generate a 169-nucleotide V3 *env* fragment in a highly sensitive triple-nested PCR strategy, utilizing 40 cycles per round. The nucleotide (nt) numbers represent their position relative to the SIV/17E-Fr strain:

Round 1:	Forward 5′-GAACTAGAGCAGAAAA TAGAACTT-3′	nt 7439–7463
	Reverse 5′-CTGGGATGTTTGAC AATG-3′	nt 7700–7683
	262-bp PCR product	
Round 2:	Forward 5′-TTTACTGGCATGGTA GGG-3′	nt 7466–7484
	Reverse 5′-CTGCTTCACCTCTTTTATT GCATC-3′	nt 7680–7656
	215-bp PCR product	
Round 3:	Forward 5′-TAGGACTATAATTAGTTT AAATAAGT-3′	nt 7488–7514
	Reverse5′-CTTCCATTTTCCTCCAAAC′	nt 7656–7638
	169-bp PCR product	

First-stage amplification was carried out in 30-μl reactions containing 1 × Reaction Buffer (Roche Diagnostics, Basel, Switzerland), containing 670 mM

Tris-HCl pH 8.8, 166 mM $(NH_4)_2SO_4$, 4.5% Triton X-100, and 2 mg/ml gelatin), 3.0 mM $MgCl_2$, 200 μM each dNTP, 0.30 μM each primer, 2 units of Expand high-fidelity DNA polymerase (Roche Diagnostics), 3 μl DNA, and water to a final volume of 30 μl. The thermal cycling consisted of an initial denaturation at 94°C for 3 min, followed by 40 cycles of amplification (94°C for 30 s, 50°C for 30 s, and 72°C for 30 s), with a final extension at 72°C for 7 min. The second- and third-round amplifications were carried out with 3 μl of the first-stage PCR product as a template. Reagent conditions and the thermal cycling were as above.

The sensitivity of the triple-nested PCR to detect SIV V3 *env* DNA was determined by using plasmid p239 SpE3' (obtained from Dr. Ronald Desrosiers through the NIH AIDS Research and Reference Reagent Program). The plasmid, of known concentration, was used as a template in the triple-nested PCR. The sensitivity of our triple-nested PCR was one or more copies of SIV V3 *env* DNA per reaction. However, at these low numbers, it is possible that DNA from an infected cell may not be aliquoted into the PCR reaction. For this reason, cell populations were collected in duplicate (e.g., two collections of astrocytes per macaque) and the triple-nested PCR was performed on each duplicate cell population at least three times to increase the frequency of detection. Integrity of DNA samples was established by performing a similar highly sensitive PCR analysis of cellular GAPDH levels, as previously described (Thompson *et al*, 2004).

PCR amplification of SIV V1 env *DNA*

A double-nested PCR was performed on DNA extracted from the cell populations to amplify SIV *env* V1 DNA sequences. V1 *env* sequences were amplified from genomic DNA prepared from LM-captured cell populations. Platinum PCR SuperMix (Invitrogen, Carlsbad, California) was used to generate a 483-bp nucleotide V1 *env* fragment in a double-nested PCR, using 40 cycles per round. The nt numbers represent their position relative to the SIV/17E-Fr strain:

Round 1:	Forward 5′-AGGAATGCGACAAT TCCCCT-3′	nt 6709–6728
	Reverse 5′-TCCATCATCCT TGTGCATGAAG-3′ 698-bp PCR product	nt 7406–7385
Round 2:	Forward 5′-CAGTCACAGAACA GGCAATAGA-3′	nt 6845–6866
	Reverse 5′-TAAGCAAAGCATAA CCTGGCGGT-3′ 483-bp PCR product	nt 7327–7305

First-stage amplification was carried out in 50-μl reactions containing 45 μl of Platinum PCR SuperMix (Invitrogen) (containing 22 units/ml *Taq* DNA polymerase with Platinum *Taq* Antibody, 22 mM Tris-HCl (pH 8.4), 55 mM KCl, 1.65 mM $MgCl_2$, 220 μM each dNTP, 0.5 μl (1.25 U) *pfu* DNA polymerase (Stratagene, La Jolla, California), 1 μM each primer, and 4 μl of DNA for a final volume of 50 μl. The thermal cycling consisted of an initial denaturation at 94°C for 3 min, followed by 40 cycles of amplification (94°C for 30 s, 50°C for 30 s, and 72°C for 30 s), with a final extension at 72°C for 7 min. The second-round amplification was carried out with 3 μl of the first-stage PCR product as a template. Reagent conditions and the thermal cycling were as above.

Cloning and sequences analysis of SIV V3 and V1 env *DNA*

The products of at least two independent PCR reactions were pooled and cloned into pGEM-T Easy (Promega, Madison, Wisconsin) for V3 *env* DNA or the TOPO TA cloning kit (with pCR 2.1-TOPO vector) (Invitrogen) for V1 *env* DNA, according to the manufacturer's protocol. Multiple V3 *env* clones and V1 *env* clones were sequenced by Applied Genetic Diagnostics, Melbourne University (Parkville, Australia) and Agencourt Bioscience Corporation (Beverly, Massachusetts), respectively. Sequences were aligned against SIVmac239 and the initial inoculated viruses SIV/17E-Fr and SIV/DeltaB670 and amino acid sequences generated using DNAMAN software (Lynnon, Quebec, Canada) or Geneious software (Biomatters, Auckland, New Zealand).

Declaration of interest: The authors report no conflicts of interest. The authors alone are responsible for the content and writing of the paper.

References

Anthony IC, Ramage SN, Carnie FW, Simmonds P, Bell JE (2005). Does drug abuse alter microglial phenotype and cell turnover in the context of advancing HIV infection? *Neuropathol Appl Neurobiol* **31:** 325–338.

Babas T, Dewitt JB, Mankowski JL, Tarwater PM, Clements JE, Zink MC (2006). Progressive selection for neurovirulent genotypes in the brain of SIV-infected macaques. *AIDS* **20:** 197–205.

Babas T, Munoz D, Mankowski JL, Tarwater PM, Clements JE, Zink MC (2003). Role of microglial cells in selective replication of simian immunodeficiency genotypes in the brain. *J Virol* **77:** 208–216.

Bechmann I, Kwidzinski E, Kovac AD, Simburger E, Horvath T, Gimsa U, Dirnagl U, Priller J, Nitsch R (2001). Turnover of rat brain perivascular cells. *Exp Neurol* **168:** 242–249.

Bell JE (2004). An update on the neuropathology of HIV in the HAART era. *Histopathology* **45:** 549–559.

Bell JE, Anthony IC, Simmonds P (2006). Impact of HIV on regional and cellular organisation of the brain. *Curr HIV Res* **4:** 249–257.

Bonavia A, Bullock BT, Gisselman KM, Margulies BJ, Clements JE (2005). A single amino acid change and truncated TM are sufficient for simian immunodeficiency virus to enter cells using CCR5 in a CD4-independent pathway. *Virology* **341:** 12–23.

Chakrabarti L, Hyrtel M, Maire MA, Vazeux R, Dormont D, Montagnier L, Hurtel B (1991). Early viral replication in the brain of SIV-infected Rhesus monkeys. *Am J Path* **139:** 1273–1280.

Churchill MJ, Gorry PR, Cowley D, lal L, Sonza S, Purcell DF, Thompson KA, Gabuzda D, McArthur JC, Pardo CA, Wesselingh SL (2006). Use of laser capture microdissection to detect integrated HIV-1 DNA in macrophages and astrocytes from autopsy brain tissue. *J NeuroVirol* **12:** 146–152.

Clarke JN, Lake JA, Burrell CJ, Wesselingh SL, Gorry PR, Peng L (2006). Novel pathway of human immunodeficiency virus type 1 uptake and release in astrocytes. *Virology* **348:** 141–155.

Clay CC, Rodrigues DS, Ho YS, Fallert BA, Janatpour K, Reinhart TA, Esser U (2007). Neuroinvasion of fluorescein-positive monocytes in acute simian immunodeficiency virus infection. *J Virol* **81:** 12040–12048.

Clements JE, Anderson MG, Zink MC, Joag SV, Narayan O (1994). The SIV model of AIDS encephalopathy. Role of neurotropic viruses in diseases. In: *HIV, AIDS and the brain*, Price RW, Perry SW (eds). New York: Raven Press. pp. 147–157.

Clements JE, Babas T, Mankowski JL, Suryanarayana K, Piatak M Jr, Tarwater PM, Lifson JD, Zink MC (2002). The central nervous system as a reservoir for simian immunodeficiency virus (SIV): steady-state levels of SIV DNA in brain from acute through asymptomatic Infection. *J Infect Dis* **186:** 905–913.

Clements JE, Zink MC (1996). Molecular biology and pathogenesis of animal lentivirus infections. *Clin Microbiol Rev* **9:** 100–117.

Dore GJ, Correll PK, Li Y, Kaldor JM, Cooper DA, Brew BJ (1999). Changes to AIDS dementia complex in the era of highly active antiretroviral therapy. *AIDS* **13:** 1249–53.

Flaherty MT, Hauer DA, Mankowski JL, Zink MC, Clements JE (1997). Molecular and biological characterization of a neurovirulent molecular clone of simian immunodeficiency virus. *J Virol* **71:** 5790–5798.

Galea I, Palin K, Newman TA, Van Rooijen N, Perry VH, Boche D (2005). Mannose receptor expression specifically reveals perivascular macrophages in normal, injured, and diseased mouse brain. *Glia* **49:** 375–384.

Gonzalez-Scarano F, Martin-Garcia J (2005). The neuropathogenesis of AIDS. *Nat Rev Immunol* **5:** 69–81.

Gray F, Scaravilli F, Everall I, Chretien F, An S, Boche D, Adle-Biassette H, Wingertsmann L, Durigon M, Hurtrel B, Chiodi F, Bell JE, Lantos P (1996). Neuropathology of early HIV-1 infection. *Brain Path* **6:** 1–15.

Hulette CM, Downey BT, Burger PC (1992). Macrophage markers in diagnostic neuropathology. *Am J Surg Path* **16:** 493–499.

Iacono RF, Berria MI (1999). Cell differentiation increases astrocyte phagocytic activity. A quantitative analysis of both GFAP labeling and PAS-stained yeast cells. *Medicina (Mex)* **59:** 171–175.

Kalmar B, Kittel A, Lemmens R, Kornyei Z, Madarasz E (2001). Cultured astrocytes react to LPS with increased cyclooxygenase activity and phagocytosis. *Neurochem Int* **38:** 453–461.

Kim WK, Alvarez X, Fisher J, Bronfin B, Westmoreland S, McLaurin J, Williams K (2006). CD163 identifies perivascular macrophages in normal and viral encephalitic brains and potential precursors to perivascular macrophages in blood. *Am J Pathol* **168:** 822–834.

Kreutzberg GW, Blakemore WF, Graaber MB (1997). Cellular pathology in the central nervous system. In: *Greenfield's neuropathology*, Graham DI, Lantos PL (eds). New York: Oxford University Press. pp. 126–137.

Laast VA, Pardo CA, Tarwater PM, Queen SE, Reinhart TA, Ghosh M, Adams RJ, Zink MC, Mankowski JL (2007). Pathogenesis of simian immunodeficiency virus-induced alterations in macaque trigeminal ganglia. *J Neuropathol Exp Neurol* **66:** 26–34.

Liu Y, Liu H, Kim BO, Gattone VH, Li J, Nath A, Blum J, He JJ (2004). CD4-independent infection of astrocytes by human immunodeficiency virus type 1: requirement for the human mannose receptor. *J Virol* **78:** 4120–4133.

Mankowski JL, Flaherty MT, Spelman JP, Hauer DA, Didier PJ, Amedee AM, Murphey-Corb M, Kirstein LM, Munoz A, Clements JE, Zink MC (1997). Pathogenesis of simian immunodeficiency virus encephalitis: viral determinants of neurovirulence. *J Virol* **71:** 6055–6060.

Mankowski JL, Spelman JP, Ressetar HG, Strandberg JD, Laterra J, Carter DL, Clements JE, Zink MC (1994). Neurovirulent simian immunodeficiency virus replicates productively in endothelial cells of the central nervous system in vivo and in vitro. *J Virol* **68:** 8202–8208.

Overholser ED, Coleman GD, Bennett JL, Casaday RJ, Zink MC, Barber SA, Clements JE (2003). Expression of simian immunodeficiency virus Nef in astorcytes during acute and terminal infection and requirement of Nef for optimal replication of neurovirulent SIV in vitro. *J Virol* **77:** 6855–6866.

Petito CK, Chen H, Mastri AR, Torres-Munoz J, Roberts B, Wood C (1999). HIV infection of choroid plexus in AIDS and asymptomatic HIV-infected patients suggests that the choroid plexus may be a reservoir of productive infection. *J NeuroVirol* **5:** 670–677.

Rothenaigner I, Kramer S, Ziegler M, Wolff H, Kleinschmidt A, Brack-Werner R (2007). Long-term HIV-1 infection of neural progenitor populations. *AIDS* **21:** 2271–2281.

Ryzhova EV, Crino P, Shawver L, Westmoreland SV, Lackner AA, Gonzalez-Scarano F (2002). Simian immunodeficiency virus encephalitis: analysis of envelope sequences from individual brain multinucleated giant cells and tissue samples. *Virology* **297:** 57–67.

Sacktor N (2002). The epidemiology of human immunodeficiency virus-associated neurological disease in the era of highly active antiretroviral therapy. *J NeuroVirol* **8:** 115–121.

Schuetze K, Becker I, Becker KF, Thalhammer S, Strack R, Heckl WM, Bohm M, Posl H (1997). Cut out or poke in—the key to the world of single genes: laser micromanipulation as a valuable tool on the look-out for the origin of disease. *Genet Anal* **14:** 1–8.

Schwartz L, Civitello L, Dunn-Pirio A, Ryschkewitsch S, Berry E, Cavert W, Kinzel N, Lawrence DMP, Hazra R,

Major EO (2007). Evidence of human immunodeficiency virus type 1 infection of nestin-positive neural progenitors in archival pediatric brain tissue. *J NeuroVirol* **13:** 274–283.

Sieczkarski SB, Whittaker GR (2002). Dissecting virus entry via endocytosis. *J Gen Virol* **83:** 1535–1545.

Speth C, Dierich MP, Sopperb S (2005). HIV-infection of the central nervous system: the tightrope walk of innate immunity. *Mol Immunol* **42:** 213–228.

Subramanian S, Bourdette DN, Corless C, Vandenbark AA, Offner H, Jones RE (2001). T lymphocytes promote the development of bone marrow-derived APC in the central nervous system. *J Immunol* **166:** 370–376.

Thompson KA, Churchill MJ, Gorry PR, Stervjoski J, Oerlichs RB, Wesselingh SL, McLean CA (2004). Astrocyte specific viral strains in HIV dementia. *Ann Neurol* **56:** 873–877.

Thompson KA, McArthur JC, Wesselingh SL (2001). Correlation between neurological progression and astrocyte apoptosis in HIV-associated dementia. *Ann Neurol* **49:** 745–752.

Trillo-Pazos G, Diamanturos A, Rislove L, Menza T, Chao W, Belem P, Sadiq S, Morgello S, Sharer L, Volsky DJ (2003). Detection of HIV-1 DNA in microglia/macrophages, astroyctes and neurons isolated from brain tissue with HIV-1 encephalitis by laser capture microdissection. *Brain Pathol* **13:** 144–154.

Williams KC, Corey S, Westmoreland SV, Pauley D, Knight H, deBakker C, Alvarez X, Lackner AA (2001). Perivascular macrophages are the primary cell type productively infected by simian immunodeficiency virus in the brains of macaques: implications for the neuropathogenesis of AIDS. *J Exp Med* **193:** 905–916.

Zink MC, Amedee AM, Mankowski JL, Craig L, Didier PJ, Carter DL, Munoz A, Murphey-Corb M, Clements JE (1997). Pathogenesis of SIV encephalitis. Selection and replication of neurovirulent SIV. *Am J Pathol* **151:** 793–803.

Zink MC, Spelman JP, Robinson RB, Clements JE (1998). SIV infection of macaques—modeling the progression to AIDS dementia. *J NeuroVirol* **4:** 249–259.

Zink MC, Suryanarayana K, Mankowski JL, Shen A, Piatak M, Spelman JP, Carter DL, Adams RJ, Lifson JD, Clements JE (1999). High viral load in the cerebrospinal fluid and brain correlates with severity of simian immunodeficiency virus encephalitis. *J Virol* **73:** 10480–10488.

This paper was first published online on iFirst on 9 July 2009.